DYNAMICS OF BIMOLECULAR REACTIONS IN SOLUTION

Andrew J. Orr-Ewing

School of Chemistry, University of Bristol, Cantock's Close, Bristol BS8 1TS, UK

02 June 2014

Tel: +44 117 9287672

e-mail: a.orr-ewing@bristol.ac.uk

Table of Contents

ABSTRACT

Mechanisms of bimolecular chemical reactions in solution are amenable to study on picosecond timescales, both by transient absorption spectroscopy and by computer simulation. The dynamics of exothermic reactions of CN radicals, and of Cl and F atoms with organic solutes in commonly used solvents are contrasted with the corresponding dynamics in the gas phase. Many characteristics of the gas-phase reaction dynamics persist in solution, such as efficient energy release to specific vibrational modes of the products. However, additional complexities associated with the presence of the solvent are open to investigation. These features of liquid-phase reactions include the role of solvent-solute complexes, solvent caging, coupling of the product motions to the solvent bath, thermalization of internally excited reaction products, incipient hydrogen bond formation, and involvement of charge-separated states that arise from proton transfer.

Keywords: radical, liquid, ultrafast, vibrational spectroscopy.

Running title: Bimolecular reactions in solution

List of Acronyms

DMB: 2,3-dimethylbut-2-ene

EVB: empirical valence bond

fs: femtosecond

IR: infrared

PES: potential energy surface

PMF: potential of mean force

ps: picosecond

THF: tetrahydrofuran

TRIR: time-resolved infrared

UV: ultraviolet

WLC: white-light continuum

1. INTRODUCTION

Liquid solvents provide a medium for many important reactions in chemical synthesis, industrial processing, environmental chemistry, and biological function. However, dissecting the mechanisms of reactions in liquids to understand the influences of solute-solvent interactions at various stages along a reaction pathway is a considerable challenge. Complexities arise from the fluxional nature of the solvent bath, which changes the intermolecular interactions experienced by the reacting species on timescales on the order of 100 fs (1-3). Initial conditions for a reaction, such as collision energies and reactant quantum states populated, are ill-defined because of rapid and continuous exchange of energy with the surrounding solvent. Information on the flow of excess energy of a reaction into specific degrees of vibrational, rotational or translational motion of the products will also be quickly washed out in a liquid-phase environment. At first glance, studying reactions in solution therefore appears to present few opportunities for penetrating insights when compared with experimental studies of collision dynamics in the gas phase. Molecular beam and laser spectroscopy techniques, for example, provide highly controlled single-collision conditions under which many reaction mechanisms have been stripped down to provide quantitative understanding of all aspects of the gas-phase chemical dynamics (4-6). This review seeks to demonstrate that, with recent progress, comparable dynamical information can now be deduced for bimolecular reactions in solution.

A simple starting point to picture the mechanism of a bimolecular reaction in solution considers diffusive approach of reagents to form an encounter pair, followed by a reactive step (7). In the scheme of reactions (1), (-1) and (2), a radical $A\cdot$ interacts with a molecule B, $[AB\cdot]$ is the encounter pair, and rate coefficients for each step are denoted by k:

$$A\cdot + B \xrightarrow{k_1} [AB\cdot] \qquad (1)$$

$$[AB\cdot] \xrightarrow{k_{-1}} A\cdot + B \qquad (-1)$$

$$[AB\cdot] \xrightarrow{k_2} products \qquad (2)$$

The overall reaction rate may be controlled by activation to surmount an energy barrier, or in the absence of any significant barrier, may be limited by the rate of diffusive encounter of the reactants. Exothermic reactions with low barriers present an opportunity to study the effect of the solvent on the mechanism of reactive step (2) because the dynamics may be sufficiently fast to outstrip coupling of the excess energy into solvent modes. Under these circumstances, transient spectroscopy of the reaction products can observe the deposition of the energy released by the reaction to the internal degrees of freedom of the products and the subsequent flow of this energy to the solvent bath (8; 9). Information on solvent modifications to the reaction mechanism then derives from comparison with the corresponding chemical dynamics under single-collision conditions in the gas phase, and with computer simulations of the reaction dynamics (10).

This article reviews recent progress with this strategy for study of bimolecular reactions in solution. Initiation by photodissociating a precursor molecule, using an actinic laser pulse, generates a reactive radical species that promptly forms the encounter pair [*AB*·]. The photodissociation step must be a fast (sub-picosecond) source of these labile radicals to ensure the observed kinetics are determined by the bimolecular reaction of interest, but this review does not consider in detail the extensive body of prior work on photodissociation and recombination dynamics in solution (3; 11). Instead, the emphasis is on chemical reaction dynamics of neutral species on the ground electronic potential energy

surface (PES), mimicking in solution many comprehensive investigations of the dynamics of gas-phase bimolecular reactions. Although the systems chosen for review involve uncharged species, the same principles might apply to important classes of ionic reactions, such as nucleophilic substitution (S_N1 and S_N2) mechanisms (12-16). Moreover, polar solvent stabilization of charge-separated states might promote a switch from initially neutral reagents to ionic reaction pathways.

The chosen method of spectroscopic monitoring must be sensitive to the internal energy content of the newly forming molecules. Transient infra-red absorption spectroscopy offers sub-picosecond time resolution, vibrational mode and state specificity, and reasonable sensitivity to low-concentration reaction products (17). In principle, transient spectroscopic methods based on Raman spectroscopy are alternatives to IR absorption (18), but have not yet been successfully applied to the types of chemical dynamics considered here. This article therefore concentrates on experimental time-resolved infra-red (TRIR) absorption studies, supplemented by transient UV/visible absorption, and complementary computational investigations of the chemical dynamics. Transient absorption techniques have also been successfully applied to the study of ultrafast dynamics of excited-state electron and proton transfer, and of isomerization reactions in solution, but these topics were the subject of recent reviews by Vauthey (19; 20) and are not considered further here. Complementary ultrafast dynamics experiments on bimolecular reactions in the gas phase are scarce because of the difficulty of overcoming the intervals between collisions in this more rarefied environment. Some progress has been made through the use of dimers and clusters at low temperatures in molecular beam expansions (21). However, most gas-phase studies have concentrated on interpretation of asymptotic properties of kinetic and internal energy

release, preferred directions of product scattering, and rotational or electronic angular momentum polarization to infer the forces acting at the transition state (TS) and in the post-TS regions of the PES (4-6).

Consideration is first given to a number of processes specific to reactions in solution, before reviewing reaction classes that have been the subject of intensive recent study (22). The solvent can stabilize or destabilize the TS relative to reactants or products, and therefore modify the height of any energy barrier to reaction and the reaction rate by, for example, dielectric effects. However, the focus here is on the dynamical features illustrated in Figure 1: (i) the reactant precursor chosen for photolytic release of reactive free radicals; (ii) the competition between removal of these labile radicals by reaction and geminate recombination; (iii) the role of complexes between reactants and solvent molecules; (iv) the effects of confinement by a solvent shell; and (v) the competing timescales for chemical reaction, post-reaction equilibration of internally excited products, and reorientation and restructuring of the solvent shell to provide equilibrated solvation of the new reaction products. Some of these processes can be studied independently of the reactive events, using methods such as transient electronic or vibrational spectroscopy of a solute (3; 23), or THz spectroscopy of solvent-solute interactions (24), which helps to unravel the interconnected dynamical processes occurring during a reactive encounter.

2. FROM PHOTO-INITIATION TO CHEMICAL REACTION

Studying chemical reaction mechanisms in solution on the femto to nanosecond timescales requires initiation at a very well-defined instant. One convenient approach is to photolyse a

stable precursor molecule, present as a co-solute; homolytic bond cleavage liberates a reactive radical species, denoted by $A\cdot$ in reactions (1) and (2). The co-reactant *B* may be a second solute, or a solvent molecule. In the latter case, diffusion is unnecessary to form an encounter pair [$AB\cdot$], but if *B* is a dilute co-solute, there may be some time delay associated with diffusion before the onset of reaction, which limits the ultimate time resolution of the experimental study of process (2). This section considers the steps in the process of photo-initiation of reaction, the intermediate species involved, and the timescales for various contributing dynamical processes that affect the experimental observations. The sub-sections broadly follow the processes illustrated in Figure 1.

2.1 PHOTOLYTIC RADICAL SOURCES

The first requirement for an experimental study of radical reaction dynamics in solution is a precursor molecule that releases the required radical following absorption of ultraviolet or visible light. The precursor should be unreactive with any co-solutes and the solvent, which imposes some significant constraints, as discussed further below. Moreover, the photo-excited precursor should release the desired radical on a timescale that is short compared to the duration of the bimolecular reaction under study. Spectroscopic signatures of the photodissociation and radical formation are therefore desirable to observe the production and reactive consumption of the radical. Two types of spectroscopic transition have successfully been exploited, either a transition of the radical itself (typically an electronic excitation, e.g. the $B \leftarrow X$ band of the CN radical (25)) or a charge-transfer band between the radical and the solvent. A white-light continuum (WLC), produced by focusing the fundamental output from an amplified Titanium-Sapphire laser into a material such as CaF_2,

is a convenient broadband source for transient electronic absorption spectroscopy (26; 27). WLCs typically span wavelengths from the near infra-red to the near UV ($\lambda \geq 320$ nm), although shorter wavelengths can be generated.

Some solvents are photochemically active at UV wavelengths typically chosen for radical formation and produce complexes or isomers that contribute transient absorption bands in the UV and visible spectral regions. For example, several halogenated solvents are known to release a halogen atom photochemically and to undergo geminate recombination to either the parent molecule or a higher energy isomeric form (28-34), as illustrated here by CCl_4:

$$CCl_4 \rightarrow CCl_3 + Cl \qquad (3)$$

$$Cl + CCl_3 \rightarrow CCl_4 \text{ or } \textit{iso}\text{-Cl-ClCCl}_2 \qquad (4)$$

The Cl atom can be observed via a charge-transfer band in which UV absorption at wavelengths around 330 nm excites an electron from the solvent to the Cl atom. The *iso*-Cl-$ClCCl_2$ species has a Cl-Cl-C bonding motif, with considerable [Cl^---CCl_3^+] ion-pair character. It has a strong, broad absorption band spanning much of the visible region, and this band grows in as the charge transfer band associated with liberated Cl atoms decays (31).

The radical species created by the homolytic bond fission can be internally excited in electronic, vibrational or rotational degrees of freedom. An extreme example is the very high rotational excitation of CN radicals from UV photolysis of ICN (35; 36). These rotationally hot radicals perturb the surrounding solvent shell and take a few picoseconds to lose their excess rotational energy and equilibrate with the solvent. Newly formed radicals will thermalize through interaction with the surrounding solvent and may form complexes that are bound with respect to an isolated radical and solvent molecule by more than the

average thermal energy (37-41). These complexes, instead of the isolated radical, may be the species involved in many radical reactions in solution, and are discussed further in section 2.3 SOLVENT-SOLUTE COMPLEXES.

Numerous photodissociation processes have been studied in solution, and several precursor molecules identified as well-suited for release of radicals for subsequent bimolecular reactions. The first such precursor proposed was UV photolysis of ICN to release CN radicals (42), and the dissociation dynamics of ICN have since been extensively studied in a range of solvents (25; 35; 43-47). Similarly, UV photolysis of alkyl iodides such as CH_3I will produce alkyl radicals, although these have yet to be used in reactive studies. Photolysis of dissolved Cl_2 has been used to examine reactions of Cl atoms with various organic molecules (48-50) but is reactive with unsaturated organic molecules, as are other plausible Cl-atom precursors such as oxalyl chloride. Recent studies of Cl atom reactions therefore used 2-photon excitation at 267 nm and dissociation of a chlorinated solvent (e.g. CCl_4, $CHCl_3$ or CH_2Cl_2) as a convenient, if less efficient, source of Cl atoms (49-51). One-photon UV photolysis of bromoalkanes is a similar route to Br-atom production (30; 34), although Br_2 photodissociation might prove more effective. Section 3.3 F-ATOM REACTIONS WITH ORGANIC SOLVENTS reviews recent developments in the study of F-atom reactions in solution. Organofluorine compounds are not susceptible to the same strategy used to generate Cl or Br atoms because of the difficulty of photolytic cleavage of C-F bonds. Instead, UV photolysis of XeF_2 (52) has proved to be a practical source of F atoms. However, XeF_2 is a powerful fluorinating agent (53), which severely restricts the choices of solvents and co-solutes used that can be used in F-atom reaction dynamics studies.

Given the small number of species in the foregoing survey, there is a clear need to extend the range of photolytic radical sources for further experiments of the type reviewed here. For example, convenient precursors and spectroscopic signatures are desirable for OH radicals, O atoms and ionic species to complement investigations of their gas-phase reactions.

2.2 REACTION VERSUS RECOMBINATION

Selection of a radical precursor must take into account the consequences of competition between the reactive removal process of interest and radical loss by geminate recombination. For example, although ICN photolysis at 266-nm is a useful method for production of CN radicals, the I + CN photoproducts can undergo rapid geminate recombination to ICN or INC isomers (25; 43; 47; 54; 55). If the recombination kinetics are fast, they can out-compete bimolecular reactions of the CN. Kinetic models used to fit experimental measurements of the rates of radical reactions should therefore incorporate the geminate recombination pathway. Analogous processes occur for other photolytic radical sources and for photolysis of halogenated solvents, as illustrated by CCl_4 in equations (3) and (4).

In many cases, the geminate recombination can be observed experimentally alongside reactive pathways. Continuing with the example of ICN, UV photolysis in an organic solvent reduces the IR absorption on the C-N stretching mode of ICN at 2176 cm^{-1}. This “bleach” of the ICN absorption band partially recovers on a picosecond timescale because of CN + I geminate recombination, and a second band assigned to the INC isomer develops at 2065

cm^{-1} (54; 55). These changes in IR absorption can be monitored simultaneously with the 2095 cm^{-1} C-N stretching mode of HCN.

2.3 SOLVENT-SOLUTE COMPLEXES

If a photolytically generated radical evades geminate recombination, it may react directly with the solvent or a co-solute molecule, or form a complex with a solvent molecule. Complexes may range from weakly associating species, confined in close proximity by a solvent cage, to more strongly associated dimers that can diffuse as a pair through the solvent, albeit with the possibility of rapid exchange of solvent molecule partner. Complexes of these types have been implicated in the chemistry of Cl atoms in chlorinated solvents (37-39; 49; 50), Br atoms in bromoform (28; 30; 34), and CN radicals in dichloromethane (40; 41; 54; 55). A bridged complex of a CN radical with CH_2Cl_2, in which the radical coordinates to both an H and a Cl atom of a solvent molecule, was calculated to be bound by 1540 cm^{-1} (40). This extra stabilization of a labile radical influences barrier heights and the dynamics of bimolecular reactions; therefore a CN may have to avoid, or escape from, the complex to react. Related effects have been carefully characterized in the gas phase, by spectroscopy of small molecular or ionic clusters (56; 57). For example, the energetics and dynamics of the S_N2 reaction of OH^- with CH_3I are profoundly changed by addition of one or two "solvent" water molecules to the OH^- anion (14).

The radical-solvent complexes can have distinct spectroscopic signatures that allow their time-evolution to be followed by transient spectroscopy. CN radical reactions in dichloromethane provide a good example: Rose et al. reported observation of a feature at 2037 cm^{-1} in dichloromethane solutions, close in wavenumber to the stretching frequency of

a gas-phase CN radical, that showed time-dependence consistent with CN-solvent complex formation following photodissociation of ICN in solution (54; 55). This complex band is also observed in chloroform, but is absent in tetrahydrofuran solutions, suggesting that THF does not complex as effectively with a CN radical. Close proximity of a radical or atom to a solvent molecule may also enhance charge transfer bands such as those seen in the UV for Cl atoms in chlorinated solvents (31; 49; 50).

The full role these complexes play in the subsequent reaction dynamics remains to be established. If the stabilization energy of the complex is substantial, reaction pathways may alter or close. For example, Crowther et al. argued that the bridged CN-solvent complex in dichloromethane solutions preferentially reacts to form ClCN, whereas a more weakly interacting linear complex also eliminates HCN. The bridged complex contributes more significantly to bimolecular reactions with added organic solutes (40; 41). However, computer simulations of the dynamics of CN radicals with cyclohexane in dichloromethane reproduce quantitatively many of the experimental observations without explicit incorporation of CN-solvent complexes (10), suggesting that much of the observed reactivity might be driven by uncomplexed, or weakly solvent-associated radicals.

2.4 SOLVENT CAGING AND CAGE ESCAPE

The solvent shell around a photo-excited precursor molecule promotes rapid thermalization of any kinetic energy released by the molecular dissociation. It can also confine the photo-generated radical pair in close proximity, sometimes with consequences for transient absorption bands, as is the case for F—XeF pairs from XeF_2 photolysis (52). At concentrations of the co-solute *B* of approximately 1 M, on average the first solvent shell

contains perhaps only one *B* molecule. There will then be competition between direct reaction with this nearest neighbour *B* and escape from the initial solvent cage, followed by diffusion into the bulk liquid until a different *B* molecule is encountered. The study by Abou-Chahine et al. of Cl atom reactions with 2,3-dimethylbut-2-ene (DMB) resolved these "in-cage" and "in-bulk" reaction pathways from the time-dependent build-up of HCl products (51), and similar behaviour is apparent in the reaction of Cl atoms with pentane and other organic molecules (49; 50).

The solvent cage also has a role to play in the post-reaction regime. As Glowacki et al. demonstrated, the vibrational relaxation dynamics of HCN and cyclohexyl radicals, formed from exothermic reaction of CN radicals with cyclohexane and confined together within a solvent cage, differ from those for separated HCN molecules in solution (8). The vibrational modes of the cyclohexyl radical couple to the modes of the nearby HCN and provide an efficient route for relaxation of the internally hot HCN born from the reaction. After ~20 ps, the two co-products have diffused apart and this relaxation pathway closes, leaving only the less efficient coupling of the HCN to the modes of the solvent bath.

2.5 TIMESCALES FOR CHEMICAL REACTION AND PRODUCT EQUILIBRATION

Once an encounter complex [*AB*·] has formed and has sufficient energy to surmount any activation barrier, reaction can occur on timescales as short as 100 fs. The chemical reaction itself is unlikely to limit the time resolution of the experiment; instead, diffusion may be the limiting factor. To observe dynamics with 1 ps time resolution or shorter, the co-reactant may need to be present at high concentrations, or be the solvent itself, to minimize diffusion times. The chemical systems reviewed in section 3. RADICAL-MOLECULE

REACTIONS IN SOLUTION have negligible energy barriers to reaction so that activation of an encounter complex is not rate-determining. However, these reactions have so far been studied at times $\geq$ 1 ps, restricting observations to properties of the newly formed reaction products from which shorter time dynamics are inferred.

The understanding developed from gas-phase studies of reactive scattering provides a starting point to think about solution-phase reactions. Signatures of particular chemical dynamics might include efficient partitioning of the excess energy of reaction to vibrational, rotational or translational degrees of freedom of the products (4; 5; 58). In solution, free rotational and translational motions are hindered, so rotation and translation induced by forces acting along the reaction path will be rapidly quenched by the solvent. However, nascent vibrational motions can persist over timescales from a few ps to a few hundred ps, depending on the strength of coupling of the solute and solvent vibrational modes (23). Observation of any specific deposition of energy into product vibrations therefore requires spectroscopic probes fast enough to compete with vibrational energy transfer to the bath. The very short timescales for translational and rotational diffusion must also be surpassed if experiments are to observe restructuring of the solvent shell around the emerging products, re-orientation of reaction products into equilibrated solvation environments, and incipient intermolecular hydrogen bond formation.

The review of reactive systems in section 3. RADICAL-MOLECULE REACTIONS IN SOLUTION shows that the most insightful measurements involve broadband transient IR spectroscopy of newly forming products. Interpretation of the time dependence of these spectra is facilitated by independent measurements of vibrational relaxation time constants (using IR-pump and IR-probe experiments (9; 23; 51; 59)) and the kinetics of removal of reagents (e.g.

with transient UV/visible absorption spectroscopy). However, polarization measurements of the decay of anisotropy, as used in photodissociation experiments (35; 36) to study loss of orientational correlation, have no obvious analogue in bimolecular reactions. Not only does the diffusion required in step (1) of the general reaction scheme obscure the precise time for onset of reaction (2), but directional information imprinted by the polarization of the excitation laser used to generate reactive radicals is lost within one or two collisions of these radicals with the solvent shell.

2.6 ANALYSIS OF KINETIC AND DYNAMICAL DATA

Decomposition of transient IR and UV/visible spectra gives time-resolved concentrations of products that can be fitted to kinetic models. If reaction products are distributed over two or more vibrational levels, the IR band intensities depend on both differences in population between spectroscopically connected levels and the squares of the transition dipole moments, which scale with vibrational quantum number. Smoluchowski theory offers one method for analysis and interpretation of the time-dependent concentrations (60; 61), and incorporates loss of reagents by both diffusive reaction and geminate recombination. Crim and coworkers successfully employed a version of Smoluchowski theory in which fits to concentration-dependent data yielded values of parameters such as reaction rate coefficients, recombination radii, and recombination yields (3; 40; 41; 49; 50; 62). For more complicated chemical processes, such as those with branching between product states, analytical or numerical integration of a kinetic scheme is more appropriate. However, kinetic schemes can contain a large number of rate coefficients, and the fits may be under-determined unless additional constraints can be applied. Values of selected rate

coefficients, measured independently using alternative experimental methods, provide such constraints. For example, vibrational relaxation rates of internally excited product molecules can be measured using IR-pump and IR-probe experiments for dilute solutions of the molecule of interest (9; 51; 54). For a harmonic oscillator, Landau-Teller theory predicts that vibrational relaxation rates from v+1 $\rightarrow$ v should scale linearly with v (23), but this approximation breaks down if there are accidental resonances with solvent modes. Total loss rates of reagent radicals can be derived from transient UV/visible spectra of charge-transfer or electronic absorption bands, and the derived rate coefficients used to constrain the sum of rate coefficients for all loss pathways of the radical. Ultimately, a chosen kinetic model should account for the time dependences of all species observed in the transient IR and UV/vis spectra (63).

3. RADICAL-MOLECULE REACTIONS IN SOLUTION

Exothermic reactions of atomic and molecular radicals with organic molecules in which a hydrogen atom is transferred are proving to be exemplars from which much can be learned about chemical dynamics in solution. Study of similar H-atom transfer reactions contributed to much of our current understanding of isolated molecule reactions in the gas phase. This section reviews examples taken from a growing literature for experimental and computational studies of reactions of CN radicals, Cl atoms and F atoms in organic solvents.

3.1 CN RADICAL REACTIONS WITH ORGANIC SOLUTES

Reactions of CN radicals with organic molecules have proven to be fertile ground for study of chemical dynamics in liquids (8-10; 54; 55; 64). They also offer ample opportunity to contrast the dynamics in solution with those in the gas phase. Early work by Benjamin and Wilson (42), and subsequent experiments by Hochstrasser and coworkers (65) provided much of the inspiration for the work discussed in this section.

Infra-red emission and absorption studies of CN radical reactions with various hydrocarbons provide a clear picture of the gas-phase dynamics (66-71). These exothermic reactions have early transition states, resulting in considerable vibrational excitation in the C-H bond of the newly formed HCN. Classical trajectory calculations by Glowacki et al. duplicated these experimental observations and also accounted for the reported excitation of the HCN bending mode: the transition state has a flat potential for displacements along the angular coordinate that maps into the HCN bend, allowing abstraction to occur over angles significantly displaced from the collinear minimum energy pathway (10).

The 1989 paper by Benjamin and Wilson proposed that experimental studies of ICN photolysis in solution would be a fruitful way to explore reaction dynamics in liquids (42). This proposal stimulated experimental investigations of ICN dissociation and recombination dynamics by the groups of Bradforth, Keiding and Zewail (25; 35; 36; 43; 46). Computational studies by Benjamin and Stratt (36; 44; 45; 47) helped to expose interesting dynamical phenomena, including a breakdown of linear response behaviour for highly rotationally excited CN photofragments. However, Raftery et al. were the first to use time-resolved IR absorption spectroscopy to observe the production of HCN following photolysis of ICN in

$CHCl_3$, and also monitored DCN from $CDCl_3$ (65). At a probe wavelength corresponding to the fundamental C-H stretching band, the time constant for rise of the HCN signal was 194 $\pm$ 20 ps, and the HCN was deduced to form exclusively in its vibrational ground state. However, in $CDCl_3$, and at an IR probe wavelength corresponding to the C-D stretching mode of DCN, first hints were reported of production of vibrationally hot products. Approximately 20% of the DCN products were argued to form with one quantum of excitation in the C-D stretch, consistent with an early transition state and despite the collisional environment of the solution.

Crim and coworkers followed the reactions of CN radicals in solution both by observation of the loss of intensity in the CN (B – X) electronic absorption band at 400 nm, and by the growth of intensity on the C-H stretching fundamental band of HCN (40; 41). In the case of the CN + pentane reaction in CH_2Cl_2, the incommensurate time constants obtained from the two spectroscopic methods suggested a role for intermediate species. Linear and bridged forms of CN-solvent complexes were invoked to account for the disparate time constants, and fits to a model incorporating Smoluchowski theory for diffusive reactions and geminate recombination satisfactorily described observed kinetic data for several chloroalkane solvents and organic solutes.

The measurements of Crim and coworkers used a narrow spread of wavelengths around 3260 cm^{-1} in the IR probe pulse to observe build-up of HCN. Subsequent experiments by Greaves et al. (9) exploited the broadband IR pulses available from the ULTRA laser system at the UK Central Laser Facility. The broadband IR radiation was dispersed onto a 128-pixel array detector to give spectral resolution of ~4 cm^{-1} per pixel over 500 cm^{-1}. Figure 2 shows a representative broadband IR absorption spectrum following UV photolysis of ICN in a 5%

solution of methanol in dichloromethane. In this case, the absorption was measured at wavenumbers around 2100 cm^{-1} and is shown for one selected time delay between the UV pulse and the IR probe pulse. This spectral region is rich in transient features, and these are assigned to CN-solvent complexes (centered at 2043 cm^{-1}), a CH_3OH bleach (2044 cm^{-1}) caused by reactive removal, INC (2065 cm^{-1}), HCN (2085 cm^{-1}), two CH_2Cl_2 bleaches (2053 and 2126 cm^{-1}), and the bleach of the C-N mode of ICN (2164 cm^{-1}). Careful spectral fitting (63) separates the time-dependences of these various bands, allowing a detailed kinetic model to be constructed of the competing removal processes for CN radicals in this ICN/MeOH/CH_2Cl_2 solution.

The experiments of Greaves et al. on the reaction of CN radicals with cyclohexane in chlorinated solvents monitored both the fundamental (v_3=1 ← v_3=0) and hot (v_3=2 ← v_3=1) bands of the ν_3 C-H stretching mode of HCN centered at respective wavenumbers of 3260 and 3160 cm^{-1} (9; 54; 55; 64). Simultaneous observation of vibrational ground and excited states of HCN demonstrated unambiguously that 70 – 80% of the HCN forms vibrationally excited with one quantum of C-H stretch and up to two quanta of bending excitation. The subsequent vibrational relaxation controls the rise time of the HCN fundamental band absorption, accounting for the discrepancy in kinetics of CN loss and HCN formation reported by Crim and coworkers. The vibrational relaxation time constant depends on the choice of solvent, but is about 150 ps in $CHCl_3$ and CH_2Cl_2. The vibrational-mode specificity observed in solution is the same as for the gas-phase dynamics, with excitation of the bend and C-H stretching modes while the C-N stretch is a spectator mode that takes up no excess energy. However, the overall vibrational energy content of the newly formed HCN is lower than for the products of the same reaction in the gas phase (71): Few and Hancock reported

HCN chemiluminescence following CN reaction with cyclohexane under low pressure conditions and spectral analysis demonstrated substantial population of HCN(v_3=2).

Computer simulations of the reaction revealed further subtle features of the dynamics. The simulations used an accurate empirical valence bond (EVB) representation of the potential energy surface (72; 73) and explicit treatment of the solvent with molecular mechanics force fields (8; 10). This computational approach is now incorporated in the CHARMM suite of programs (74). Rapid loss of internal energy from vibrationally hot HCN over the first 20 ps results from efficient energy transfer to the partner cyclohexyl radical co-product. At these early times, solvent caging keeps the HCN and cyclohexyl products in close proximity and provides a more favourable route for energy flow than to the solvent bath, but this route is disrupted by diffusive separation.

When normal cyclohexane is replaced by d_{12}-cyclohexane, the DCN products also form with substantial vibrational excitation. However, the excitation is now observed in all three vibrational modes of the molecule (55). A local mode description of the stretching vibrations is more appropriate for HCN than DCN, for which the two stretching vibrations involve coupled C-D and C-N motions. The D-atom transfer along the reaction coordinate therefore projects onto both modes of the product.

The chlorinated organic solvents used for the CN radical reactions are weakly interacting with solutes such as HCN, and the same is true for the cyclohexane co-reactant. With the benefit of hindsight, it is perhaps not surprising that the chemical dynamics in these solvents retain many of the features characteristic of isolated collisions in the gas phase. Nevertheless, the observed changes to the dynamics in solution provide valuable information on solvent modifications to reaction mechanisms. Moreover, solvents and

solutes can be selected that have larger couplings to the reaction coordinate or the newly formed products to explore the effect of stronger interactions. Two examples are discussed here, in which the cyclohexane co-reagent is replaced either by tetrahydrofuran (THF) or methanol. THF has C-H stretching modes that are close to resonant in frequency with the C-H stretching mode of HCN, and methanol is an example of a liquid which might act as a hydrogen-bond donor or acceptor with HCN.

The near resonance of a THF C-H stretching mode causes rapid energy transfer from the ν_3 vibration of HCN to the solvent bath. Rose et al. conducted experiments in which reactions of CN radicals were observed for different dilutions (0.5 – 8.2 M) of THF in a chlorinated solvent (either $CDCl_3$ or CD_2Cl_2) (54). Following ICN photolysis, the experiments monitored the C-N stretching vibration of HCN at 2073 cm^{-1}, which is adjacent to an IR band of the INC isomer centered at 2052 cm^{-1}. The kinetics of recombination to form INC and reaction to produce HCN could therefore be monitored simultaneously. Analysis of the concentration-dependent rate coefficients for HCN production gave a bimolecular rate coefficient for the CN + THF reaction of $(1.57 \pm 0.12) \times 10^{10}$ M^{-1} s^{-1}. The rapid relaxation of vibrationally excited HCN reaction products, with time constants of < 8 ps in THF/CD_2Cl_2 solutions compared to 170 ± 6 ps in cyclohexane/CD_2Cl_2 solutions, suggests stronger vibrational coupling to the solvent bath. Nevertheless, experimental evidence was obtained that the bimolecular reaction dynamics again favour HCN(v_3=1) reaction products. Simulations based on an EVB potential for the reaction and the Merck Molecular Mechanics force field reproduced the experimental observations. These simulations required adjustment of the THF force constants to bring the computed spectral bands closer to the frequencies obtained in steady-state IR spectra, demonstrating that molecular mechanics methods can

succeed in modelling the experiments as long as the vibrational force fields are correctly treated. This study indicates that near-resonance of solvent modes with newly developing vibrational modes of an emerging reaction product has greater effect asymptotically than on the post-TS region of the reaction pathway. The solvent response may not be fast enough to adjust promptly to the changes in bonding associated with the chemical reaction.

Reactions of CN radicals with methanol provide an opportunity to explore the effects of intermolecular hydrogen bonds on the chemical dynamics. Furthermore, CH_3OH has two distinct H-atom sites from which abstraction might occur, and reactions at these two sites can be distinguished by selective deuteration (CD_3OH vs CH_3OD). Interference by methanol IR absorption bands prevents experimental measurements for ICN solutions in the neat alcohol, so Grubb et al. used dilute solutions of methanol in dichloromethane in their experiments (75). The exact nature of the solvent structure around a dissociating ICN molecule becomes ill-defined in such an approach, with the likelihood of microscopic partitioning of methanol and dichloromethane molecules, giving methanol clusters (76). However, bleach signals of the type evident in figure 2 appear in the transient IR experiments corresponding to reactive removal of both CH_3OH and CH_2Cl_2. Preliminary measurements that simultaneously probe C-N stretching modes of DCN and HCN by broadband IR absorption show a preference for HCN formation in partially deuterated methanol samples, suggesting pronounced kinetic isotope effects that are the subject of ongoing investigation.

3.2 Cl-ATOM REACTIONS WITH ORGANIC SOLUTES

Reactions of chlorine atoms with organic molecules are well established as benchmark systems for study of the dynamics of reactions of polyatomic molecules in the gas phase (77; 78). Under isolated reactive collision conditions, these reactions exemplify bond specific chemistry, vibrational-mode-specific dynamics, the effects of impact parameter on scattering, and how post-transition state complexes can influence product energy disposal (79-85). In recent work on reactions of Cl atoms with alkenes, Suits and coworkers (86-88) and Preston et al. (89) examined competition between two pathways for HCl production, direct H-atom abstraction and reaction mediated by addition of a Cl atom to the C=C bond. This latter pathway was shown to occur via large-amplitude Cl-atom dynamics that access a loose transition state connecting the addition complex with the direct abstraction path.

Hochstrasser's study of Cl atom reactions with cyclohexane was the first use of transient infra-red absorption spectroscopy to follow a bimolecular chemical reaction in solution on ps timescales (48). Cl_2 dissolved in cyclohexane was photolysed by a short UV pulse, and IR pulses a few tens of picoseconds in duration observed the formation of HCl (or DCl from d_{12}-cyclohexane) products. A rate coefficient was reported that was ~14 times slower than the corresponding reaction in the gas phase.

Cl-atoms can also be generated photolytically by absorption of two 267-nm photons by chlorinated solvents. Crim and coworkers used this approach, as well as dissolved Cl_2 photodissociation, to extend the work of Hochstrasser to reactions of Cl atoms with numerous organic solutes (3; 49; 50; 62). While transient IR absorption effectively probes the production of HCl, transient UV-visible absorption spectroscopy conveniently monitors the removal of Cl atoms through spectral signatures of their complexes with solvent

molecules (31; 49; 50). Analysis of the time dependence of a charge-transfer band of the solvent-Cl complex, using a model based on Smoluchowski theory to account for diffusion and geminate recombination (60; 61), gave bimolecular rate coefficients that depended strongly on the nature of the organic solute. The relative rates were successfully explained using structure-activity relationships based on gas-phase Cl-atom reactions. For the nearly diffusion-limited reaction of Cl with pentane in either CH_2Cl_2 or CCl_4, reaction rates and geminate recombination fractions depended on solvent viscosity.

Broadband transient IR absorption spectroscopy allowed Abou-Chahine et al. to explore the dynamics of Cl-atom reactions in addition to the kinetics (51). Reaction of Cl atoms with 2,3-dimethylbut-2-ene is sufficiently exothermic to populate HCl(v=0, 1 and 2) vibrational levels in the gas phase because of the formation of a resonance-stabilized allylic radical co-product (89). Figure 3 shows representative transient IR spectra for HCl from the Cl + DMB reaction in $CDCl_3$, which demonstrate that the direct abstraction pathway known from the gas phase is still active in solution. However, addition of Cl to the C=C bond is unlikely to yield HCl because of collisional stabilization of the adduct, as well as solvent-shell suppression of the large-amplitude motions that lead from the adduct to H-atom abstraction (88; 89). Not only was HCl product observed via its fundamental band at 2825 cm^{-1}, but Abou-Chahine et al. reported that for reaction in $CDCl_3$, (24$\pm$4)% of the HCl was produced in v=1. When the experiments were carried out in CCl_4, this branching to HCl(v=1) was (15$\pm$2)%. In comparison, the gas-phase reaction of Cl with propene, which is less exothermic than the Cl + DMB reaction, is estimated to produce (48$\pm$6)% HCl(v=1) products (90). At least three plausible explanations for the damped vibrational excitation seen in solution can be proposed: (i) coupling of the post-TS motions of the developing products to

the modes of the solvent bath removes energy from the nascent HCl bond; (ii) the reacting form of Cl is modified from the gas phase by complexation to one or more solvent molecules, causing a displacement of the TS later along the reaction coordinate; (iii) the addition-mediated pathway for abstraction of an H-atom, known to occur in the gas phase but suppressed in solution, is responsible for much of the HCl vibrational excitation. Recent experimental and computational studies have greatly clarified the nature of the gas-phase chemical dynamics for Cl + alkene reactions (88; 89). Resolution of the causes of the changes that occur in solution now requires corresponding computer simulations with explicit treatment of the solvent molecules.

3.3 F-ATOM REACTIONS WITH ORGANIC SOLVENTS

F-atom reactions with H_2, methane, water and various H/D isotopologues demonstrate rich and subtle dynamics in the gas phase. For example, at low collision energies, tunnelling through the reaction barrier contributes significantly to the reaction cross section (91), and the scattering shows signatures of Feschbach resonances on the product side of the TS (92; 93). Production of HF from F+H_2 and F+CH_4 reactions is highly exothermic, with a significant fraction of the available energy appearing as HF vibrational excitation (94-96). Nesbitt and coworkers extended the experimental investigation of F-atom reaction dynamics to scattering from liquid hydrocarbon surfaces (97), but until very recently there were no comparative studies in solution.

Progress in the study of F-atom reaction dynamics in liquids followed from the demonstration that 267-nm photolysis of dissolved XeF_2 serves as a prompt source of F-atoms (52). Figure 4 compares transient UV/vis and IR absorption spectra obtained

following 267-nm photolysis of XeF_2 in d_3-acetonitrile. The UV/vis spectra reveal production of XeF and XeF—F caged complexes on sub-ps timescales, and loss of the XeF—F complexes with a time constant of 4.3 ± 2.2 ps in CD_3CN (3.4 ± 2.1 ps in CD_2Cl_2). This loss was attributed mostly to removal of F atoms by reaction with the solvent. The XeF is stable on the microsecond timescale in acetonitrile (98), but reacts with d_2-dichloromethane with a time constant of 800 ± 200 ps (52; 99).

Time-resolved IR spectroscopy following XeF_2 photolysis in liquid CD_3CN or CD_2Cl_2 provides many further insights (99). The central frequency of the fundamental band of DF lies at 2480 cm^{-1} in acetonitrile solution, and is a broad, unstructured feature. As figure 4 shows, this band grows within ~30 ps after UV excitation of dissolved XeF_2, but components of the TRIR spectra shift both to higher and lower wavenumber during this time. Deconvolution of these shifting spectral bands revealed that DF forms with up to 2 quanta of vibrational excitation at early times, and thermalizes with time constants of about 3 ps for single-quantum vibrational relaxation steps. This vibrational relaxation accounts for the shift of the spectrum to higher wavenumber at early times, because of the substantial anharmonicity of the DF vibrational mode. Computer simulations by Glowacki et al. quantitatively reproduce these experimental observations and their time constants (100). The shift of the fundamental band by 160 cm^{-1} to lower wavenumber occurs with a time constant of 10 ps and is indicative of changes to the solvation environment of the DF, although the simulations suggest incipient hydrogen bonding is much faster and occurs on sub-picosecond timescales. The 10-ps time constant is 3 to 4 times slower than the measured orientation correlation time for molecules in liquid water (101; 102). Although acetonitrile responds very rapidly to changes in solute geometry or polarity (103), the F-

atom reaction occurs more quickly, and the newly formed DF undergoes rotational and translation diffusion before settling into an equilibrated interaction with the solvent. This type of non-adiabatic picture of the solvent response to reaction was discussed by Orr-Ewing in the context of Kramers (104) and Grote-Hynes (105; 106) theories of reaction rates in solution (22). Although the reaction occurs on a PES that is neutral and covalent in character, about 90 kJ mol^{-1} of vibrational excitation of the products brings them to potential energies where charge-separated states deriving from proton transfer can influence the reaction. Correct treatment of the reaction pathway in computer simulations therefore requires inclusion of these proton-transfer states in the Hamiltonian.

As was the case for solution phase CN reactions with various organic molecules, and Cl reactions with 2,3-dimethylbut-2-ene, the DF products of F + CD_3CN and CD_2Cl_2 reactions are vibrationally excited. However, in all these examples, the extent of vibrational excitation is less than is observed for the corresponding reactions in the gas phase. Setser and coworkers reported DF(v=4 and 5) products dominate the gas-phase reaction of F atoms with CD_2Cl_2 (107), and measurements of the F + CH_3CN reaction suggest similar outcomes for F + CD_3CN (108). Possible reasons for lower vibrational excitation of reaction products in solution were proposed in section 3.2 Cl-ATOM REACTIONS WITH ORGANIC SOLUTES, and similar arguments apply to the F atom reactions. The coupling of the DF to the solvent is strong, as demonstrated by the short vibrational relaxation time constants (3 – 4 ps) obtained from IR-pump and IR-probe measurements. This coupling may affect the DF even as it is forming, providing a damping force for the nascent bond. The F atom can complex to XeF or a solvent molecule (52), which might modify the PES for reaction. However, the simulations recover the measured timescales without explicit inclusion of XeF

(100), so perhaps this possibility can be discounted. The nuclear dynamics across the PES may also be constrained by the solvent cage, thus favouring a restricted subset of the geometries sampled in the gas phase reactions.

4. CONTRASTING DYNAMICS IN THE GAS AND LIQUID PHASES

A broad ambition of the research reviewed here is to understand how a liquid environment modifies the chemical dynamics from those occurring under isolated conditions in the gas phase (3). Glowacki et al. contrasted computed PESs and potentials of mean force (PMFs) for CN radical reactions with hydrocarbons in both environments and reported only minor modifications induced by representative organic solvents (8; 10). On the other hand, solvent-solute interactions substantially modify the energy profile of an S_N2 reaction between an anion and a neutral molecule in solution from that for the same reaction in the gas phase (12; 13; 15). Comparisons can also be drawn between experimental measurements of the outcomes of bimolecular reactions in gases and in solution, and Table 1 summarizes the information available to date.

The data presented in the table show a consistent trend: the solvent partially, but incompletely, quenches the nascent vibrational energy of reaction products. In the examples given, the vibrational excitation of the indicated product is approximately half that of the gas-phase reaction. Although mean collision energies generally differ in the two environments, the energy available to the products is dominated by the exothermicity of the reaction and so the comparisons should be instructive.

Several effects may be responsible for this product vibrational damping in the liquid phase, and these ideas were introduced in earlier sections. The solvent may couple to the reaction coordinate and to orthogonal degrees of freedom of the reacting molecules in the post-TS region where chemical energy release occurs and vibrational excitation develops in the nascent products. This coupling can be regarded as a post-TS friction that suppresses vibrational excitation, and will be promoted by (near) resonances of solvent modes with the developing modes of the reaction products. Alternatively, the reactants may form complexes with solvent molecules that lower their potential energy, and therefore affect the location of the TS along the reaction coordinate, moving it later than for the reaction of an uncomplexed radical. These ideas can be tested by accurate computer simulations of the reaction, for example by computing reactive trajectories in which a radical is coordinated to a single solvent molecule to form a representative complex. The simulations performed to date include explicit solvent molecules and can therefore incorporate reactant-solvent complexes, but are based on PESs computed for the "bare" radical reaction.

Reactions of F atoms with hydrocarbons at the gas-liquid interface, shown in the bottom row of Table 1, also result in lower product vibrational excitation than for the corresponding gas-phase reactions (97; 109). However, the dynamical origins are different from those for reactions in bulk liquids. In the case of surface scattering, two mechanisms compete: direct reaction followed by prompt scattering back to the gas phase produces vibrationally hot products via dynamics very similar to the gas-phase reaction, whereas products trapped within the surface of the liquid thermalize before desorbing.

A recent perspective article (22) connected the observations from studies of CN radical reactions in solution with the models for solvent effects incorporated into Kramers (1; 104)

and Grote-Hynes (105; 106) theories of chemical reaction rates in solution. The CN reactions appear to be well described by a regime in which solvent collisions do not significantly impair motion along the reaction coordinate and through the TS. In the language of Kramers theory, this description corresponds to a low solvent friction regime. Passage through the TS is faster than, or comparable to, solvent collision and reorientation times, and the solvent does not adjust to an equilibrated configuration on the timescale of the reaction. This analysis suggests a TS that is not optimally stabilized by solvent interactions, corresponding to non-adiabatic solvation within the framework of Grote-Hynes theory. Gas-phase like dynamics therefore persist in solution, but with some damping of the nascent vibrational excitation of the emerging products through coupling to the solvent (a post-TS friction or equilibration). The solvent plays further important roles by caging reactants and products (8), influencing the stereochemistry of the reaction by constraining geometries of approach to the TS, and stabilizing pre- and post-TS reaction complexes, corresponding, for example, to formation of new H-bonds. All of these effects depend on the nature of the chosen solvent.

5. FUTURE DEVELOPMENTS AND CONCLUSIONS

The experimental and computational studies reviewed in section 3. RADICAL-MOLECULE REACTIONS IN SOLUTION examined bimolecular radical reactions in representative organic solvents, and at ambient temperatures. Although these solvents have different polarities, and some are hydrogen-bonding in character, systematic studies have not yet been performed of the effects of solvent properties such as viscosity, structure and intermolecular interactions. Temperature variation will affect the viscosity, and may also provide further understanding of the role of solvent complexes, and perhaps the origins of

isotopic effects in H- versus D-atom transfer reactions. With increasing use of ionic liquids in chemical synthesis, and of supercritical fluids in various applications, study of chemical dynamics in these media may furnish new insights. Mechanistic studies in water remain largely unexplored for bimolecular reactions of the type reviewed here, although various photochemical processes including dissociation and recombination have been examined by transient absorption in this most important of all liquid environments (25; 43; 110-114). H-atom transfer reactions from solvent molecules are proposed to mediate diffusion of OH radicals in water, as well as fast recombination of electrons with OH following charge-transfer to solvent by photoexcitation of hydroxide ions (115; 116). In aqueous solution, ion chemistry will be more significant than in typical organic solvents. However, study of ionic reaction mechanisms on ultrafast timescales presents challenges for the experimentalist to photo-initiate the chemistry promptly and follow reactions by transient IR spectroscopy against strong water absorption bands. One illustrative example instead used transient UV absorption to monitor the ground electronic state protonation of the $ONOO^-$ base in water (117).

Although performed on ultrafast timescales, the experimental measurements summarized in this review are asymptotic observations of the products of chemical reactions. Transient absorption spectroscopy methods are not yet directly probing passage along the reaction coordinate, but instead are using the vibrational energy content of products as a signature of the PES. Nor are the experiments monitoring the restructuring of the surrounding solvent as reactants transform to products. At the instant of crossing a transition state, newly emerging products may have higher degrees of vibrational excitation than when separated, with some coupling of the nascent products to the solvent damping this

excitation even as the reaction completes. Alternatively, the solvent may appear frozen on the timescale of the reaction, with the onset of coupling to the solvent bath only occurring once the products have formed. Better time resolution is necessary to resolve these types of pictures of the dynamics, but is limited by the timescale for formation of encounter complexes from separated reactants and the subsequent initiation of reactive events. Spectroscopic signatures of the solvent structure around ongoing chemical reactions would also provide valuable insights.

The field of study of bimolecular reaction dynamics in solution, although inspired by prescient theoretical and pioneering experimental work in the 1980s and 1990s, remains relatively unexplored. As experimental and computational capabilities improve, many new dynamical insights are emerging. In many cases, mechanisms of reactions deduced from gas-phase studies provide a valuable first picture of the dynamics in solution, but the presence of the solvent introduces many new facets to the chemistry which are now amenable to detailed investigation.

SUMMARY POINTS

1. Bimolecular reactions in liquid solutions can be studied on picosecond timescales using photodissociation of a stable precursor to release a reactive radical and time-resolved absorption spectroscopy to follow loss of reagents and formation of products. Examples include reactions of CN radicals and F and Cl atoms.
2. The reactive radicals interact with the surrounding solvent and can form radical-solvent complexes that influence the reaction mechanism.

3. Exothermic reactions release some of their excess energy to internal motions of the reaction products, and time-resolved infrared absorption spectroscopy can follow this flow of energy into vibrational modes of the products and then to the solvent bath. Comparison between the degrees of vibrational excitation of newly born products of a reaction in the gas phase and in solution reveals how the solvent modifies the potential energy landscape for the reaction and the associated nuclear dynamics from the transition state to products.
4. A combination of experimental measurements and computational simulations of the dynamics distinguishes between solvent modification of the reaction mechanism and coupling of the products of the reaction to the solvent bath modes.
5. Competition between radical loss pathways such as complexation or reaction with the solvent, reaction with a co-solute, and geminate recombination and isomerization complicate the analysis of time-dependent spectral data, and broadband absorption measurements that observe multiple species are required to unravel the competing pathways.
6. Computer simulations using accurate potential energy functions and molecular mechanics modelling of the solvent can reproduce quantitatively many of the experimental observations, but require very careful treatment of the solute-solvent interactions to capture dynamical effects correctly.
7. There is considerable scope to extend the current studies to a wider range of solvents and reactive radicals, to explore effects of solvent temperature and viscosity systematically, and to examine reactions of ions.

ACKNOWLEDGEMENTS

Financial support for the University of Bristol group from the Engineering and Physical Sciences Research Council (EPSRC, Programme Grant EP/G00224X) and the European Research Council (ERC, Advanced Grant 290966 CAPRI) is gratefully acknowledged. I am indebted to M.N.R. Ashfold, S.J. Greaves, R.A. Rose, F. Abou-Chahine, G.T. Dunning, D. Murdock, T.J. Preston, M.P. Grubb, G.M. Roberts, H. Marroux, D.R. Glowacki, J.N. Harvey, M. Towrie, G.M. Greetham, I.P. Clark, S.E. Bradforth, D.J. Nesbitt and F.F. Crim for many valuable discussions.

LITERATURE CITED

1. Nitzan A. 2006. *Chemical Dynamics in Condensed Phases*. Oxford: Oxford University Press
2. Voth GA, Hochstrasser RM. 1996. Transition state dynamics and relaxation processes in solutions: a frontier of physical chemistry. *J. Phys. Chem.* 100:13034-49
3. Elles CG, Crim FF. 2006. Connecting chemical dynamics in gases and liquids. *Annu Rev Phys Chem* 57:273-302
4. Brouard M, Vallance C. 2010. *Tutorials in Molecular Reaction Dynamics*. Cambridge: Royal Society of Chemistry
5. Levine RD. 2005. *Molecular Reaction Dynamics*. Cambridge: Cambridge University Press
6. Greaves SJ, Rose RA, Orr-Ewing AJ. 2010. Velocity map imaging of the dynamics of bimolecular chemical reactions. *Phys. Chem. Chem. Phys.* 12:9129-43
7. Pilling MJ, Seakins PW. 1995. *Reaction Kinetics* Oxford: Oxford University Press
8. Glowacki DR, Rose RA, Greaves SJ, Orr-Ewing AJ, Harvey JN. 2011. Ultrafast energy flow in the wake of solution-phase bimolecular reactions. *Nat. Chem.* 3:850-5
9. Greaves SJ, Rose RA, Oliver TAA, Glowacki DR, Ashfold MNR, et al. 2011. Vibrationally quantum-state-specific reaction dynamics of H atom abstraction by CN radical in solution. *Science* 331:1423-6
10. Glowacki DR, Orr-Ewing AJ, Harvey JN. 2011. Product energy deposition of CN + alkane H abstraction reactions in gas and solution phases. *J. Chem. Phys.* 134:214508
11. Harris SJ, Murdock D, Zhang YY, Oliver TAA, Grubb MP, et al. 2013. Comparing molecular photofragmentation dynamics in the gas and liquid phases. *Phys. Chem. Chem. Phys.* 15:6567-82
12. Chen X, Regan CK, Craig SL, Krenske EH, Houk KN, et al. 2009. Steric and solvation effects in ionic S(N)2 reactions. *J. Am. Chem. Soc.* 131:16162-70
13. Vayner G, Houk KN, Jorgensen WL, Brauman JI. 2004. Steric retardation of S_N2 reactions in the gas phase and solution. *J. Am. Chem. Soc.* 126:9054-8

14. Otto R, Brox J, Trippel S, Stei M, Best T, Wester R. 2012. Single solvent molecules can affect the dynamics of substitution reactions. *Nat. Chem.* 4:534-8
15. Zhang J, Xu Y, Chen J, Wang D. 2014. A multilayered representation, quantum mechanical / molecular mechanics study of the $CH_3Cl + F^-$ reaction in aqueous solution: the reaction mechanism, solvent effects and potential of mean force. *Phys. Chem. Chem. Phys.* 16:7611-7
16. Fingerhut BP, Sailer CF, Ammer J, Riedle E, de Vivie-Riedle R. 2012. Buildup and decay of the optical absorption in the ultrafast photo-generation and reaction of benzhydryl cations in solution. *J. Phys. Chem. A* 116:11064-74
17. Greetham GM, Burgos P, Cao Q, Clark IP, Codd PS, et al. 2010. ULTRA: a unique instrument for time-resolved spectroscopy. *Appl. Spectrosc.* 64:1311-9
18. McCamant DW, Kukura P, Mathies RA. 2003. Femtosecond broadband stimulated Raman: A new approach for high-performance vibrational spectroscopy. *Appl. Spectrosc.* 57:1317-23
19. Rosspeintner A, Lang B, Vauthey E. 2013. Ultrafast photochemistry in liquids. *Annu Rev Phys Chem* 64:247-71
20. Vauthey E. 2006. Investigations of bimolecular photoinduced electron transfer reactions in polar solvents using ultrafast spectroscopy. *Journal of Photochemistry and Photobiology a-Chemistry* 179:1-12
21. Scherer NF, Khundkar LR, Bernstein RB, Zewail AH. 1987. Real-time picosecond clocking of the collision complex in a bimolecular reaction - the birth of OH from $H+CO_2$. *J Chem Phys* 87:1451-3
22. Orr-Ewing AJ. 2014. Bimolecular chemical reaction dynamics in solution. *J. Chem. Phys.* 140:090901
23. Owrutsky JC, Raftery D, Hochstrasser RM. 1994. Vibrational-relaxation dynamics in solutions. *Annu Rev Phys Chem* 45:519-55
24. Grossman M, Born B, Heyden M, Tworowski D, Fields GB, et al. 2011. Correlated structural kinetics and retarded solvent dynamics at the metalloprotease active site. *Nat. Struc. Mol. Biol.* 18:1102-U113
25. Rivera CA, Winter N, Harper RV, Benjamin I, Bradforth SE. 2011. The dynamical role of solvent on the ICN photodissociation reaction: connecting experimental observables directly with molecular dynamics simulations. *Phys. Chem. Chem. Phys.* 13:8269-83
26. Megerle U, Pugliesi I, Schriever C, Sailer CF, Riedle E. 2009. Sub-50 fs broadband absorption spectroscopy with tunable excitation: putting the analysis of ultrafast molecular dynamics on solid ground. *Appl. Phys. B* 96:215-31
27. Riedle E, Bradler M, Wenninger M, Sailer CF, Pugliesi I. 2013. Electronic transient spectroscopy from the deep UV to the NIR: unambiguous disentanglement of complex processes. *Faraday Discussions* 163:139-58
28. Carrier SL, Preston TJ, Dutta M, Crowther AC, Crim FF. 2010. Ultrafast observation of isomerization and complexation in the photolysis of bromoform in solution. *J. Phys. Chem. A* 114:1548-55
29. Preston TJ, Dutta M, Esselman BJ, Kalume A, George L, et al. 2011. Formation and relaxation dynamics of iso-CH_2Cl-I in cryogenic matrices. *J. Chem. Phys.* 135:114503
30. Preston TJ, Shaloski MA, Crim FF. 2013. Probing the photoisomerization of $CHBr_3$ and CHI_3 in solution with transient vibrational and electronic spectroscopy. *J. Phys. Chem. A* 117:2899-907
31. Abou-Chahine F, Preston TJ, Dunning GT, Orr-Ewing AJ, Greetham GM, et al. 2013. Photoisomerization and photoinduced reactions in liquid CCl_4 and $CHCl_3$. *J. Phys. Chem. A* 117:13388-98
32. El-Khoury PZ, Kwok WM, Guan X, Ma C, Phillips DL, Tarnovsky AN. 2009. Photochemistry of iodoform in methanol: formation and fate of the iso-CHI_2-I photoproduct. *Chem.Phys.Chem.* 10:1895-900

33. Kwok WM, Ma CS, Parker AW, Phillips D, Towrie M, et al. 2000. Picosecond time-resolved resonance Raman observation of the iso-CH_2I-I photoproduct from the "photoisomerization" reaction of diiodomethane in the solution phase. *J. Chem. Phys.* 113:7471-8
34. Pal SK, Mereshchenko AS, Butaeva EV, El-Khoury PZ, Tarnovsky AN. 2013. Global sampling of the photochemical reaction paths of bromoform by ultrafast deep-UV through near-IR transient absorption and ab initio multiconfigurational calculations. *J. Chem. Phys.* 138:124501
35. Moskun AC, Bradforth SE. 2003. Photodissociation of ICN in polar solvents: evidence for long lived rotational excitation in room temperature liquids. *J. Chem. Phys.* 119:4500-15
36. Moskun AC, Jailaubekov AE, Bradforth SE, Tao GH, Stratt RM. 2006. Rotational coherence and a sudden breakdown in linear response seen in room-temperature liquids. *Science* 311:1907-11
37. Chateauneuf J. 1999. Kinetic evidence for chlorine atom complexes in "noncomplexing" solvents. *J. Org. Chem.* 64:1054 - 5
38. Chateauneuf JE. 1989. Charge-transfer absorption spectra of chlorine atoms in halogenated solvents. *Chem. Phys. Lett.* 164:577-80
39. Chateauneuf JE. 1990. Direct measurement of the absolute kinetics of chlorine atom in CCl_4. *J. Am. Chem. Soc.* 112:442-4
40. Crowther AC, Carrier SL, Preston TJ, Crim FF. 2008. Time-resolved studies of CN radical reactions and the role of complexes in solution. *J. Phys. Chem. A* 112:12081-9
41. Crowther AC, Carrier SL, Preston TJ, Crim FF. 2009. Time-resolved studies of the reactions of CN radical complexes with alkanes, alcohols, and chloroalkanes. *J. Phys. Chem. A* 113:3758-64
42. Benjamin I, Wilson KR. 1989. Proposed experimental probes of chemical-reaction molecular-dynamics in solution - ICN photodissociation. *J Chem Phys* 90:4176-97
43. Larsen J, Madsen D, Poulsen JA, Poulsen TD, Keiding SR, Thogersen J. 2002. The photoisomerization of aqueous ICN studied by subpicosecond transient absorption spectroscopy. *J. Chem. Phys.* 116:7997-8005
44. Vieceli J, Chorny I, Benjamin I. 2001. Photodissociation of ICN at the liquid/vapor interface of chloroform. *J. Chem. Phys.* 115:4819-28
45. Benjamin I. 1995. Photodissociation of ICN in liquid chloroform - molecular-dynamics of ground and excited-state recombination, cage escape, and hydrogen abstraction reaction. *J. Chem. Phys.* 103:2459-71
46. Wan CZ, Gupta M, Zewail AH. 1996. Femtochemistry of ICN in liquids: dynamics of dissociation, recombination and abstraction. *Chem Phys Lett* 256:279-87
47. Winter N, Chorny I, Vieceli J, Benjamin I. 2003. Molecular dynamics study of the photodissociation and photoisomerization of ICN in water. *J. Chem. Phys.* 119:2127-43
48. Raftery D, Iannone M, Phillips CM, Hochstrasser RM. 1993. Hydrogen abstraction dynamics in solution studied by picosecond infrared-spectroscopy. *Chem. Phys. Lett.* 201:513-20
49. Sheps L, Crowther AC, Carrier SL, Crim FF. 2006. Time-resolved spectroscopic study of the reaction Cl + n-$C_5H_{12} \rightarrow$ HCl + C_5H_{11} in solution. *J. Phys. Chem. A* 110:3087-92
50. Sheps L, Crowther AC, Elles CG, Crim FF. 2005. Recombination dynamics and hydrogen abstraction reactions of chlorine radicals in solution. *J. Phys. Chem. A* 109:4296-302
51. Abou-Chahine F, Greaves SJ, Dunning GT, Orr-Ewing AJ, Greetham GM, et al. 2013. Vibrationally resolved dynamics of the reaction of Cl atoms with 2,3-dimethylbut-2-ene in chlorinated solvents. *Chem. Sci.* 4:226-37
52. Dunning GT, Preston TJ, Orr-Ewing AJ, Greaves SJ, Greetham GM, et al. 2014. Dynamics of photodissociation of XeF_2 in organic solvents, submitted.
53. Tius MA. 1995. Xenon difluoride in synthesis. *Tetrahedron* 51:6605-34

54. Rose RA, Greaves SJ, Abou-Chahine F, Glowacki DR, Oliver TAA, et al. 2012. Reaction dynamics of CN radicals with tetrahydrofuran in liquid solutions. *Phys. Chem. Chem. Phys.* 14:10424-37
55. Rose RA, Greaves SJ, Oliver TAA, Clark IP, Greetham GM, et al. 2011. Vibrationally quantum-state-specific dynamics of the reactions of CN radicals with organic molecules in solution. *J. Chem. Phys.* 134:244503
56. O'Donnell BA, Beames JM, Lester MI. 2012. Experimental characterization of the CN $X^2\Sigma^+$ + Ar and H_2 potentials via infrared-ultraviolet double resonance spectroscopy. *J. Chem. Phys.* 136:234304
57. Han JD, Heaven MC, Schnupf U, Alexander MH. 2008. Experimental and theoretical studies of the CN-Ar van der Waals complex. *J. Chem. Phys.* 128:104308
58. Polanyi JC. 1972. Concepts in reaction dynamics. *Acc. Chem. Res.* 5:161-8
59. Knudtson JT, Stephenson JC. 1984. Vibrational Relaxation of HCl in Dilute CCl_4 and CCl_3F Solutions. *Chem. Phys. Lett.* 107:385-8
60. Tachiya M. 1983. Theory of diffusion-controlled reactions - formulation of the bulk reaction-rate in terms of the pair probability. *Radiation Phys. Chem.* 21:167-75
61. Rice SA. *Diffusion-Limited Reactions; Comprehensive Chemical Kinetics 25*. New York 1985: Elsevier
62. Elles CG, Cox MJ, Barnes GL, Crim FF. 2004. Recombination and reaction dynamics following photodissociation of CH_3OCl in solution. *J. Phys. Chem. A* 108:10973 - 9
63. Grubb MP, Orr-Ewing AJ, Ashfold MNR. 2014. KOALA: a new program for the processing and decomposition of transient spectra. *Rev Sci Instrum* in press.
64. Orr-Ewing AJ, Glowacki DR, Greaves SJ, Rose RA. 2011. Chemical reaction dynamics in liquid solutions. *J. Phys. Chem. Lett.* 2:1139-44
65. Raftery D, Gooding E, Romanovsky A, Hochstrasser RM. 1994. Vibrational product state dynamics in solution-phase bimolecular reactions - transient infrared study of CN radical reactions. *J. Chem. Phys.* 101:8572-9
66. Bethardy GA, Northrup FJ, He G, Tokue I, Macdonald RG. 1998. Initial vibrational level distribution of HCN $X^1\Sigma^+(v_10v_3)$ from the $CN(X^2\Sigma^+)+H_2 \rightarrow HCN+H$ reaction. *J. Chem. Phys.* 109:4224-36
67. Bethardy GA, Northrup FJ, Macdonald RG. 1995. The initial vibrational-state distribution of HCN $X^1\Sigma^+$ $(v_1,0,v_3)$ from the reaction $CN(^2\Sigma^+)+C_2H_6 \rightarrow HCN+C_2H_5$. *J. Chem. Phys.* 102:7966-82
68. Bethardy GA, Northrup FJ, Macdonald RG. 1996. The initial vibrational level distribution and relaxation of HCN $X^1\Sigma^+$ $(v_1,0,v_3)$ in the $CN(X^2\Sigma^+)+CH_4 \rightarrow HCN+CH_3$ reaction system. *J. Chem. Phys.* 105:4533-49
69. Copeland LR, Mohammad F, Zahedi M, Volman DH, Jackson WM. 1992. Rate constants for CN reactions with hydrocarbons and the product HCN vibrational populations: examples of heavy-light-heavy abstraction reactions. *J. Chem. Phys.* 96:5817-26
70. Morris VR, Mohammad F, Valdry L, Jackson WM. 1994. Steric effects on nascent vibrational distributions of the HCN product produced in CN radical reactions with ethane, propane and chloroform. *Chem. Phys. Lett.* 220:448-54
71. Few J. 2013. *FTIR Studies of Chemical Processes*. D.Phil. Thesis, University of Oxford
72. Warshel A, Weiss RM. 1980. An empirical valence bond approach for comparing reactions in solutions and in enzymes. *J Am Chem Soc* 102:6218-26
73. Kamerlin SCL, Warshel A. 2011. The empirical valence bond model: theory and applications. *Wires Comput Mol Sci* 1:30-45
74. Brooks BR, Brooks CL, Mackerell AD, Nilsson L, Petrella RJ, et al. 2009. CHARMM: The biomolecular simulation program. *J. Comput. Chem.* 30:1545-614
75. Grubb MP, Marroux H, Roberts GM, Dunning GT, Orr-Ewing AJ. 2014. Liquid phase dynamics of the reaction of CN radicals with methanol. *In preparation*.

76. Kuen DS, Feierabend KJ. 2014. Cavity-enhanced overtone spectroscopy of methanol in aprotic solvents: probing solute-solvent interactions and self-associative behavior *J. Phys. Chem. A* 118:2942-51
77. Murray C, Orr-Ewing AJ. 2004. The dynamics of chlorine atom reactions with polyatomic organic molecules. *Int. Rev. Phys. Chem.* 23:435-82
78. Murray C, Pearce JK, Rudic S, Retail B, Orr-Ewing AJ. 2005. Stereodynamics of chlorine atom reactions with organic molecules. *J. Phys. Chem. A* 109:11093-102
79. Simpson WR, Orr-Ewing AJ, Zare RN. 1993. State-to-state differential cross-sections for the reaction $Cl(^2P_{3/2})+CH_4(v_3=1,J=1) \rightarrow HCl(v'=1,J')+CH_3$. *Chem. Phys. Lett.* 212:163-71
80. Simpson WR, Rakitzis TP, Kandel SA, Orr-Ewing AJ, Zare RN. 1995. Reaction of Cl with vibrationally excited CH_4 and CHD_3 - state-to-state differential cross-sections and steric effects for the HCl product. *J. Chem. Phys.* 103:7313-35
81. Berke AE, Volpa EH, Annesley CJ, Crim FF. 2013. The influence of translational and vibrational energy on the reaction of Cl with CH_3D. *J. Chem. Phys.* 138:224306
82. Holiday RJ, Kwon CH, Annesley CJ, Crim FF. 2006. Mode- and bond-selective reaction of $Cl(^2P_{3/2})$ with CH_3D: C-H stretch overtone excitation near 6000 cm^{-1}. *J. Chem. Phys.* 125:133101
83. Rudic S, Murray C, Ascenzi D, Anderson H, Harvey JN, Orr-Ewing AJ. 2002. The dynamics of formation of HCl products from the reaction of Cl atoms with methanol, ethanol, and dimethyl ether. *J. Chem. Phys.* 117:5692-706
84. Rudic S, Murray C, Harvey JN, Orr-Ewing AJ. 2003. The product branching and dynamics of the reaction of chlorine atoms with methylamine. *Phys. Chem. Chem. Phys.* 5:1205-12
85. Rudic S, Murray C, Harvey JN, Orr-Ewing AJ. 2004. On-the-fly ab initio trajectory calculations of the dynamics of Cl atom reactions with methane, ethane and methanol. *J. Chem. Phys.* 120:186-98
86. Estillore AD, Visger LM, Suits AG. 2010. Imaging the dynamics of chlorine atom reactions with alkenes. *J. Chem. Phys.* 133:074306
87. Joalland B, Van Camp R, Shi YY, Patel N, Suits AG. 2013. Crossed-beam slice imaging of Cl reaction dynamics with butene isomers. *J. Phys. Chem. A* 117:7589-94
88. Joalland B, Mebel A, Suits AG. 2014. Roaming dynamics in Cl + butene. *submitted*
89. Preston TJ, Dunning GT, Orr-Ewing AJ, Vazquez SA. 2014. Direct and indirect abstraction in Cl + alkene reactions. *J. Phys. Chem. A* submitted.
90. Pilgrim JS, Taatjes CA. 1997. Infrared absorption probing of the Cl+C3H6 reaction: rate coefficient for HCl production between 290 and 800 K. *J. Phys. Chem. A* 101:5776-82
91. Tizniti M, Le Picard SD, Lique F, Berteloite C, Canosa A, et al. 2014. The rate of the F + H_2 reaction at very low temperatures. *Nat. Chem.* 6:141-5
92. Dong WR, Xiao CL, Wang T, Dai DX, Yang XM, Zhang DH. 2010. Transition-state spectroscopy of partial wave resonances in the F + HD reaction. *Science* 327:1501-2
93. Qiu MH, Ren ZF, Che L, Dai DX, Harich SA, et al. 2006. Observation of Feshbach resonances in the $F+H_2 \rightarrow HF+H$ reaction. *Science* 311:1440-3
94. Neumark DM, Wodtke AM, Robinson GN, Hayden CC, Lee YT. 1985. Molecular-beam studies of the $F+H_2$ reaction. *J. Chem. Phys.* 82:3045-66
95. Neumark DM, Wodtke AM, Robinson GN, Hayden CC, Shobatake K, et al. 1985. Molecular-beam studies of the $F+D_2$ and F+HD reactions. *J. Chem. Phys.* 82:3067-77
96. Lin JJ, Zhou JG, Shiu WC, Liu KP. 2003. State-specific correlation of coincident product pairs in the $F+CD_4$ reaction. *Science* 300:966-9
97. Zolot AM, Dagdigian PJ, Nesbitt DJ. 2008. Quantum-state resolved reactive scattering at the gas-liquid interface: F plus squalane ($C_{30}H_{62}$) dynamics via high-resolution infrared absorption of nascent HF(v,J). *J. Chem. Phys.* 129:194705
98. Bucher G, Scaiano JC. 1994. Absolute rate constants for atomic fluorine in solution - characterization of reaction intermediates in the laser flash-photolysis of xenon difluoride. *J Am Chem Soc* 116:10076-9

99. Dunning GT, Glowacki DR, Preston TJ, Greaves SJ, Greetham GM, et al. 2014. Incipient hydrogen bonding between DF reaction products and solvent molecules *submitted*
100. Glowacki DR, Orr-Ewing AJ, Harvey JN. 2014. A parallel multistate framework for non-equilibrium reaction dynamics in strongly interaction organic solvents: F abstraction reactions in d-acetonitrile. *submitted*
101. Omta AW, Kropman MF, Woutersen S, Bakker HJ. 2003. Negligible effect of ions on the hydrogen-bond structure in liquid water. *Science* 301:347-9
102. Woutersen S, Bakker HJ. 1999. Resonant intermolecular transfer of vibrational energy in liquid water. *Nature* 402:507-9
103. Bagchi B, Jana B. 2010. Solvation dynamics in dipolar liquids. *Chemical Society Reviews* 39:1936-54
104. Kramers HA. 1940. Brownian motion in a field of force and the diffusion model of chemical reactions. *Physica* 7:284-304
105. Grote RF, Hynes JT. 1980. The stable states picture of chemical reactions .2. Rate constants for condensed and gas-phase reaction models. *J. Chem. Phys.* 73:2715-32
106. Grote RF, Hynes JT. 1981. Saddle-point model for atom transfer-reactions in solution. *J. Chem. Phys.* 75:2191-8
107. Wickramaaratchi MA, Setser DW, Hildebrandt H, Korbitzer B, Heydtmann H. 1985. Evaluation of HF product distributions deduced from infrared chemiluminescence .2. F-atom reactions. *Chem. Phys.* 94:109-29
108. Dehe K, Heydtmann H. 1996. HF infrared emission from the reactions of atomic fluorine with methylcyanide, methylisocyanide, dimethylsulfide and dimethyldisulfide. *Chem Phys Lett* 262:683-8
109. Whitney ES, Zolot AM, McCoy AB, Francisco JS, Nesbitt DJ. 2005. Reactive scattering dynamics in atom plus polyatomic systems: $F+C_2H_6$ -> $HF(v,J)+C_2H_5$. *J Chem Phys* 122:124310
110. Madsen A, Thomsen CL, Poulsen JA, Jensen SJK, Thogersen J, et al. 2003. Femtosecond photolysis of HOCl(aq): Dissipation of fragment kinetic energy. *J. Phys. Chem. A* 107:3606-11
111. Thogersen J, Jensen SK, Christiansen O, Keiding SR. 2004. Fast photodynamics of aqueous formic acid. *Journal of Physical Chemistry A* 108:7483-9
112. Thogersen J, Jepsen PU, Thomsen CL, Poulsen JA, Byberg JR, Keiding SR. 1997. Femtosecond photolysis of ClO_2 in aqueous solution. *J. Phys. Chem. A* 101:3317-23
113. Thomsen CL, Madsen D, Poulsen JA, Thogersen J, Jensen SJK, Keiding SR. 2001. Femtosecond photolysis of aqueous HOCl. *J. Chem. Phys.* 115:9361-9
114. Petersen C, Thogersen J, Jensen SK, Keiding SR, Sassi P. 2008. Solvent response to solute photo-dissociation. *Phys. Chem. Chem. Phys.* 10:990-5
115. Codorniu-Hernandez E, Kusalik PG. 2011. Insights into the solvation and mobility of the hydroxyl radical in aqueous solution. *J. Chem. Theo. Comput.* 7:3725-32
116. Iglev H, Fischer MK, Gliserin A, Laubereau A. 2011. Ultrafast geminate recombination after photodetachment of aqueous hydroxide. *J. Am. Chem. Soc.* 133:790-5
117. Keiding SR, Madsen D, Larsen J, Jensen SK, Thogersen J. 2004. When molecules meet: a femtosecond study of the protonation of a base. *Chem Phys Lett* 390:94-7

Chemical Reaction	Gas Phase	Liquid Solution
CN + c-C_6H_{12} → **HCN** + c-C_6H_{11}	v_{max} = 2 (C–H stretch) (71)	v_{max} = 1 (C–H stretch) in $CDCl_3$ and CD_2Cl_2 (9)
Cl + $(CH_3)_2C=C(CH_3)_2$ → **HCl** + $(CH_3)_2C=C(CH_3)(CH_2)$	v_{max} = 2 (89) v = 1 in 50% yield for Cl + propene (90)	v_{max} = 1 (in ≤ 25% yield) in $CDCl_3$ and CCl_4 (51)
F + CD_2Cl_2 → **DF** + $CDCl_2$ F + CD_3CN → **DF** + CD_2CN	v_{max} = 5 (107) $v_{max} \geq 3$ (108)	v_{max} = 2 in CD_2Cl_2 (99) v_{max} = 2 in CD_3CN (99)
	Gas Phase	Gas-Liquid Interface
F + RH → **HF** + R	F + C_2H_6 → HF + C_2H_5 f_{vib}(HF) = 56% (109)	F + squalane → HF + squalane· f_{vib}(HF) = 37% (97)

Table 1: Comparison of vibrational excitation of reaction products in the gas and liquid phases. The maximum populated vibrational level (v_{max}) is shown for the species identified in bold font. The bottom row shows a similar comparison of fractions of the available energy in product HF vibration (f_{vib}) for F-atom reactions with hydrocarbons in the gas phase and at a gas-liquid interface.

Figure 1: Schematic diagram of the processes considered here for bimolecular reactions in solution, exemplified by CN radical reaction with a hydrocarbon co-solute. UV photodissociation of ICN liberates a CN radical and an I atom (A and B). The photofragments can geminately recombine (B to A), or diffusively separate and the CN may complex to a solvent molecule (C), or react with the hydrocarbon to form internally hot (D) or thermalized (E) product species. The solvent-complexed radical may undergo similar reactions (C to D or E). Internally excited products lose their excess energy to the solvent bath (D to E), and products diffuse apart (F). Transient IR spectroscopy provides information on all of these steps.

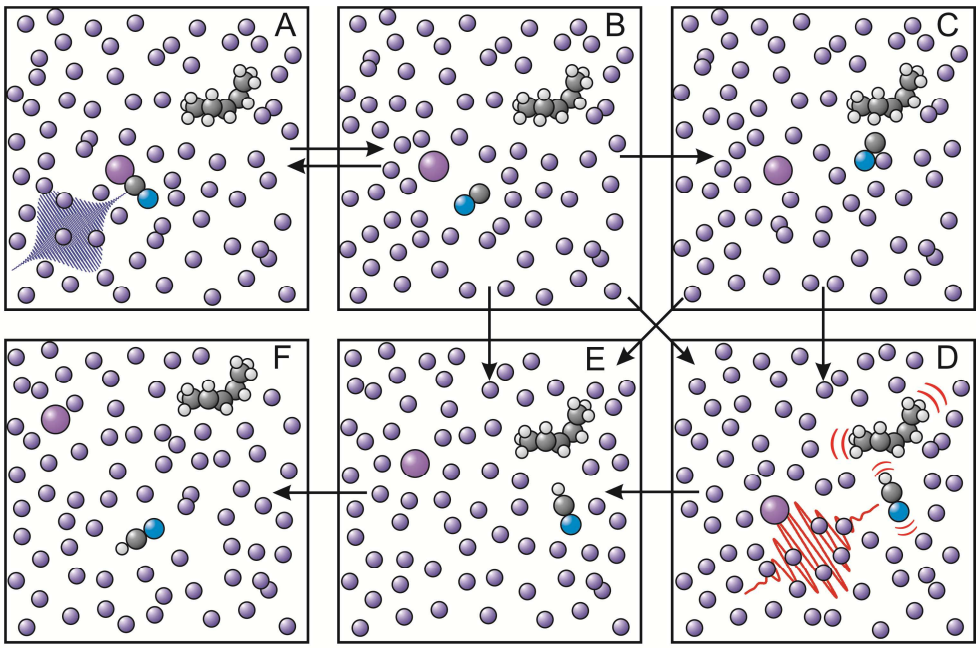

Figure 2: Broadband transient IR absorption spectrum (red line) obtained 256 ps after UV photolysis of ICN in a 5% solution of methanol in dichloromethane. The black dashed line is a fit of the experimental spectrum to contributions from absorption bands of INC, a CN-solvent complex, HCN, CH_3OH and CH_2Cl_2 as indicated. Positive peaks show products of the CN-radical chemistry, and negative peaks correspond to consumption of reagents.

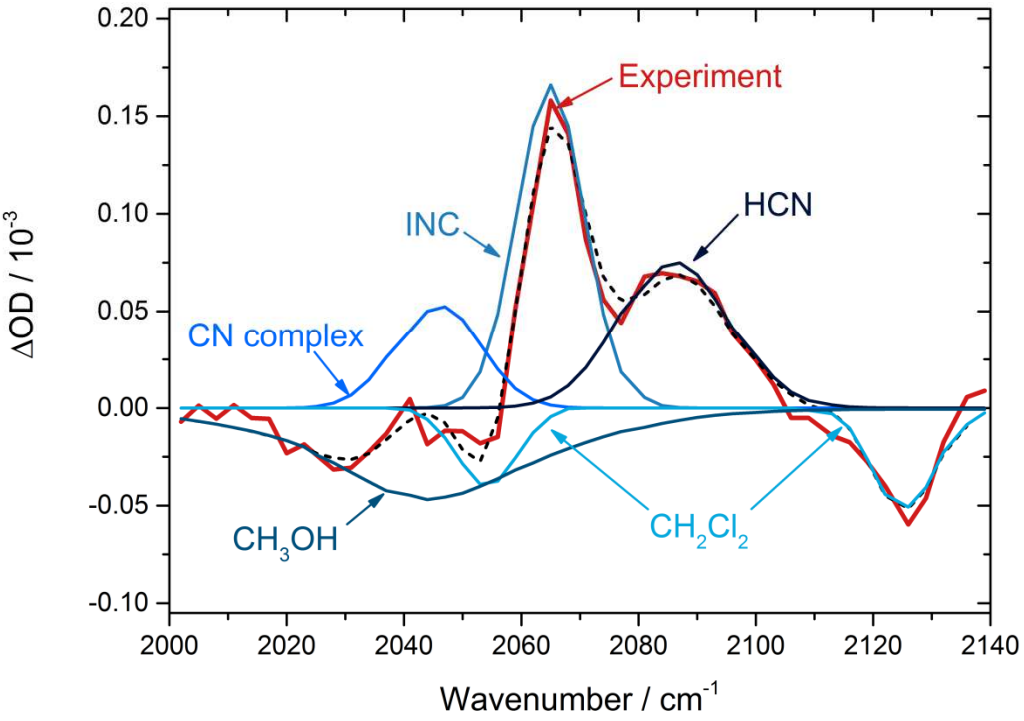

Figure 3: Time-dependent IR absorption spectra of HCl from the photoinitiated reaction of Cl atoms with 2,3-dimethylbut-2-ene in $CDCl_3$. The feature that grows at 2850 cm^{-1} is absorption by HCl(v=0) and the transient feature at 2710 cm^{-1} is assigned to HCl(v=1). The inverted solid black line is a steady-state FTIR spectrum of a solution of 2,3-dimethylbut-2-ene in $CDCl_3$. The inset key relates the colours of the spectra to the time delays between UV and IR laser pulses. The inset plot shows the time dependences of the intensities of the two absorption bands (circles) and a fit to a kinetic model (lines).

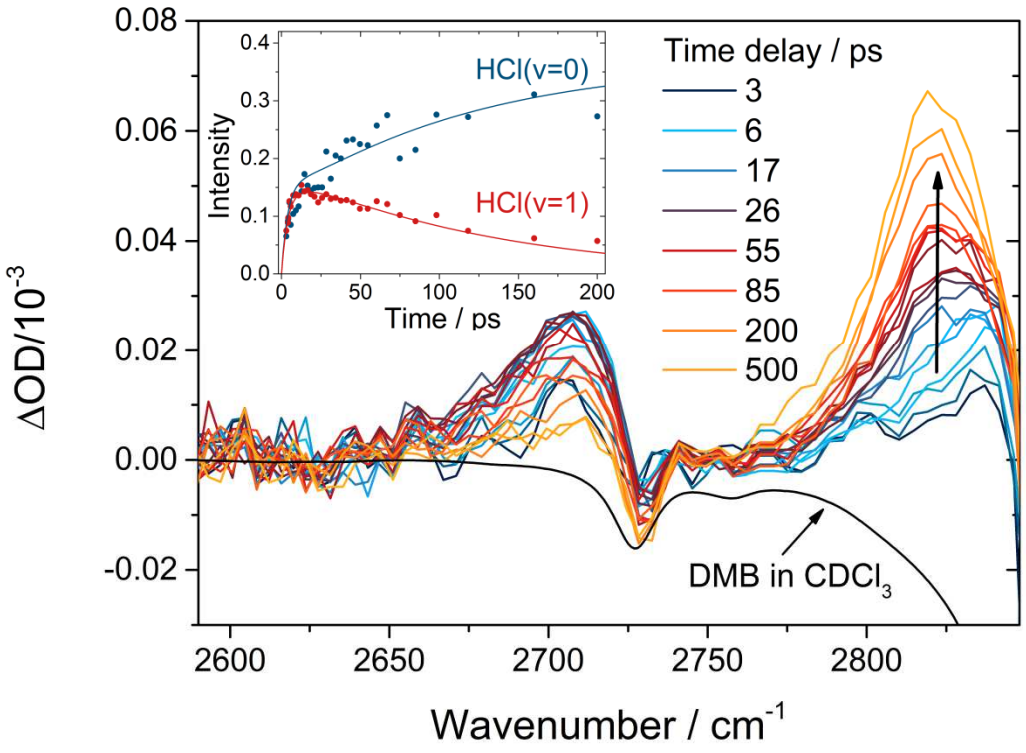

Figure 4: Transient (A) UV-visible and (B) IR absorption spectra following 267-nm photolysis of XeF_2 in CD_3CN. The keys show the colour scheme used for spectra obtained at different time delays between the UV excitation and the probe laser pulses. The band centered at 340 nm in (A) is assigned to XeF, and the shoulder at longer wavelength is attributed to F--XeF complexes. The inset shows the intensity changes of each of these spectral bands at early times. The inset to panel (B) shows the time-dependence of vibrational band absorptions by DF(v=0 and 1) that contribute to the broad feature in panel (B), together with fits to a kinetic model constrained by data from both spectra. The bold arrows highlight shifts in spectral features.